



The miRNA-34a/Sirt1/p53 pathway in a rat model of lens regeneration

Xue Bi^{1,2#}, Rui Wang^{1,2#}, Hui Song^{1,2#}, Yuchuan Wang^{1,2}, Peng Hao^{1,2}, Xuan Li^{1,2}

¹Clinical College of Ophthalmology, Tianjin Medical University, Tianjin, China; ²Tianjin Eye Institute, Tianjin Key Lab of Ophthalmology and Visual Science, Tianjin Eye Hospital, Tianjin, China

Contributions: (I) Conception and design: H Song, X Li; (II) Administrative support: X Li; (III) Provision of study materials or patients: Y Wang, P Hao; (IV) Collection and assembly of data: X Bi, R Wang; (V) Data analysis and interpretation: X Bi; (VI) Manuscript writing: All authors; (VII) Final approval of manuscript: All authors.

[#]These authors contributed equally to this work and should be considered as co-first authors.

Correspondence to: Xuan Li. Tianjin Eye Institute, Tianjin Key Lab of Ophthalmology and Visual Science, Tianjin Eye Hospital, No. 4 Gansu Road, He-ping District, Tianjin 300020, China. Email: xuanli08@yahoo.com.

Background: There are many molecular factors involved in Wolffian and corneal lens regeneration, but few in lens regeneration by lens epithelial cells (LECs) in mammals. Silent information regulator 1 (Sirt1) has a variety of physiological functions, such as a transport hub, and is involved in pathological conditions. We studied the expression of the microRNA (miRNA)-34a/Sirt1/tumor protein p53 (p53) pathway in a rat model of lens regeneration.

Methods: We performed extracapsular lens extraction in 42 healthy female Sprague-Dawley rats. Slit lamp observation was performed at 3, 7, 14, 21, 30, 60 and 90 days postoperatively, and the rats were killed humanely by cervical dislocation at 30, 60 and 90 days postoperatively to remove the eyeballs. We performed semiquantitative immunofluorescence analysis of Sirt1, p53, alpha-smooth muscle actin (α -SMA) and fibronectin (fn), and real-time fluorescence quantitative polymerase chain reaction (RT-qPCR) to detect the relative expressions of miRNA-34a, Sirt1, p53, aquaporin 0 (AQP 0), γ A-crystallin, and beaded filament structural protein 1 (BFSP1) mRNA in the lens and posterior capsule.

Results: The posterior capsule wrinkled at 3 days and it increased at 7 days. At 14 days, pearl-like opacification appeared under the capsule, with increasing shrinkage. Greater mass-like proliferators in size and number accumulated under the capsule and at the equator after 21 days. A regenerated lens developed in the central depression of the capsule at 30 days, slightly protruding from it. Despite being thickened at 60 days, the central depression persisted, with a smaller change at 90 days than at 60 days. Although the relative mRNA expression of miRNA-34a and p53 in the lens and posterior capsule decreased over time ($P=0.000$), that of Sirt1 increased ($P<0.01$). α -SMA was uniformly expressed in the crystals and gradually decreased, while fn expression gradually increased.

Conclusions: miRNA-34a expression decreased and Sirt1 expression increased during lens regeneration. Furthermore, p53 expression decreased, thus reducing apoptosis. Therefore, Sirt1 acted as a key factor in the pathway, and played a protective role in lens regeneration.

Keywords: Lens regeneration; miRNA-34a/Sirt1/p53 pathway; ophthalmology; rat model

Submitted Mar 21, 2022. Accepted for publication Jun 23, 2022.

doi: 10.21037/atm-22-2099

View this article at: <https://dx.doi.org/10.21037/atm-22-2099>

Introduction

With the development of stem cells, repair and regeneration have become the focus of tissue and organ research. Cataracts are a blind eye disease, and the currently available treatment is surgery alone. The most common surgical techniques for the treatment of cataracts are phacoemulsification and extracapsular cataract extraction. During cataract surgery, the failure to completely remove lens cells from the capsule results in an abnormal proliferation of the lens epithelial cells (LECs), which in turn may lead to posterior capsule opacification (PCO) (1). PCO is one of the most common postoperative complications, developing in 20–50% of patients 2–5 years after surgery and resulting in visual loss (2). Neodymium-doped Yttrium aluminum garnet (Nd:YAG) laser is the most commonly used method for the treatment of PCO, but despite being non-invasive, it has several complications, such as displacement or damage to the intraocular lens (IOL), iritis, intraocular pressure fluctuations, macular edema, retinal tears, or detachment (3). Based on the current limitations of cataract treatment and the postoperative complications, the use of a regenerated lens as a self-lens might be a novel avenue for future treatment (4).

Lens regeneration can be divided into the following three types according to their origin (1). (I) Wolffian lens regeneration, common in amphibians, such as newts and salamanders. It occurs in both the juvenile and adult stages. The new lens originates from pigment epithelial cells located along the dorsal rim of the iris. In contrast, the ventral rim of the iris does not have regeneration capacity. Wolffian lens regeneration is triggered by factors provided by the neural retina (5-8). (II) Corneal lens regeneration (9), whereby the new lens originates from the basal layer of the corneal epithelium, and is only observed in animals such as *Xenopus* (10,11). Corneal lens regeneration is also triggered by factors provided by the neural retina (9). (III) LEC regeneration; that is, replacement by existing LECs. This process can also be seen in mammals, such as rabbits, cats, rats (12-14). In a study on lens regeneration in rabbits, macaques, and infants, the lens was removed through a small incision of the posterior capsule, and most of the anterior capsule was retained. After 5 months, a primary lens with better transparency formed and the fundus could be clearly observed (15).

There are several molecular factors involved in Wolffian and corneal lens regeneration, such as the fibroblast growth factor (FGF) (16,17), wingless-related integration site (18,19), retinoic acid (20,21), and bone morphogenetic

protein signals (19,22), but fewer are known for lens regeneration in LECs (1).

The microRNA (miRNA)-34a/silent information regulator 1 (Sirt1)/tumor protein p53 (p53) pathway is involved in apoptosis and has been studied in LECs (23). In human LECs, anti-apoptotic factors B-cell lymphoma-2 and Sirt1 were significantly reduced by up-regulation of miRNA-34a (23). miRNA-34a is a member of the miRNA-34 family involved in apoptosis and aging (24). The coding gene of miRNA-34a is located at 1p36.2 and is expressed at a low level in several tumor tissues (25). Sirt1 has a variety of physiological functions, such as a transport hub, and is involved in pathological conditions through regulation of numerous closely related upstream miRNAs and several downstream targets that contain transcription factors that play a key role in cell survival and metabolism. Sirt1 maintains chromatin silencing and genomic stability (26), and is one of the target genes of miRNA-34a (23). Moreover, it inhibits cell death following DNA injury by antagonizing p53 acetylation (27). The upregulation of miRNA-34a expression level is associated with cataract occurrence in rats, which may be caused by down-regulation of Sirt1 protein (28). Sirt1 protects LECs from oxidative stress by inhibiting the p53 pathway (29). Therefore, it can be inferred that in miRNA-34a/Sirt1/p53 pathway, miRNA-34a reversely regulates Sirt1, which in turn reversely regulates p53. During lens regeneration, LECs showed a state of proliferation, which may be due to the inhibition of p53 pathway, and miRNA-34a/Sirt1/p53 pathway may be involved in this process. No studies have been conducted on the expression of miRNA-34a/Sirt1/p53 pathway in lens regeneration. In this study, we aimed to investigate the expression changes of miRNA-34a, Sirt1 and p53 in a rat model of regenerated lens, and to compare the expressions of alpha-smooth muscle actin (α -SMA) and fibronectin (fn), markers of tissue fibrosis, and aquaporin 0 (AQP 0), γ A-crystallin, beaded filament structural protein 1 (BFSP1), markers of lens fibers. To explore the possible role of miRNA-34a/Sirt1/p53 pathway in lens regeneration. We present the following article in accordance with the ARRIVE reporting checklist (available at <https://atm.amegroups.com/article/view/10.21037/atm-22-2099/rc>).

Methods

Ethics approval

Animal experiments were performed under a project license

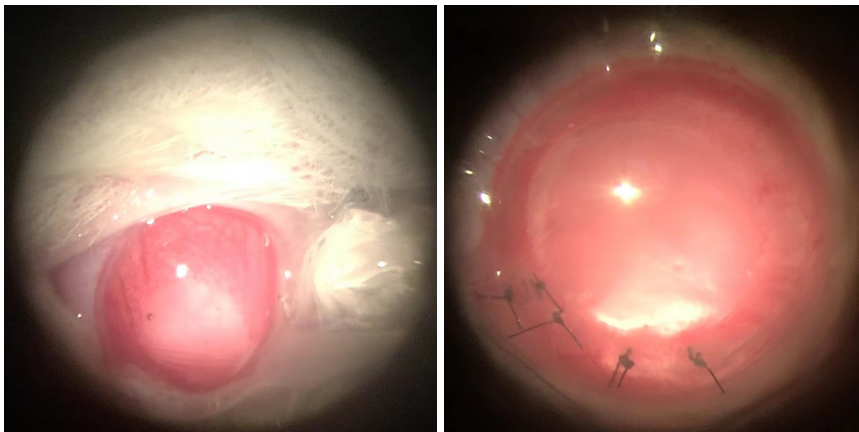


Figure 1 Model-making process. After the incision was enlarged, the lens nucleus and cortex were delivered, and the incision was sutured with 10/0 sutures. At the end of the operation, the anterior chamber had formed, with little bleeding, no obvious iris incarceration, and a clear posterior capsule.

(No. NKYY-DWLL-2020-098) granted by the Animal Ethical and Welfare Committees of Nankai Hospital, in compliance with the Guide for the Care and Use of Laboratory Animals of Nankai Hospital. The experimental animals are raised and killed in the animal room of Nankai Hospital, and Nankai Hospital and Tianjin Eye Hospital is a medical union. A protocol was prepared before the study without registration.

Animals

We acquired 42 healthy, adult, clean-grade female Sprague-Dawley rats (randomly selected the same sex to prevent reproduction), 8–10 weeks old, and weighing 200–220 g, from Beijing HFK Bio-science Co. (Beijing, China). Groups of five rats were raised together in a plastic cage (15×30×45 cm³). The rats were housed in a 12-h light/dark cycle at 22–24 °C with 40–50% humidity. Food and water were available ad libitum. The rats were divided into three groups of 14 rats each using a computer based random order generator. The right and left eyes were the experimental and control groups, respectively. The experimental unit is an eye. Our animal experiments followed the statement by the Association for Research in Vision on using animals in ophthalmic and visual studies.

Establishing the animal model

Extracapsular excision of lens in rats was performed by the same operator who was aware of the group allocation at the

different stages of the experiment. At 30 min before the operation, each rat was weighed, and 2% intraabdominal pentobarbital sodium (40 mg/kg) was injected. Following induction of general anesthesia, the rats were fixed to the operating table. The right eye underwent mydriasis, conjunctival capsule washing, disinfection, and surface anesthesia. A corneal incision was made using a 2.8-mm puncture knife, followed by injection of a viscoelastic agent to maintain the anterior chamber. The anterior capsule, approximately 2.5 mm in diameter, was torn off at the center, and the cortex and nucleus were separated using water. After expanding along the corneal incision to ~120°, the lens and cortex were extracted by compression. The corneal incision was sutured to form a watertight anterior chamber. At the end of surgery, levofloxacin eye drops, tobramycin dexamethasone eye ointment, and atropine eye gel were applied. Replace the clean bedding for the postsurgical rat. The operation lasted in half an hour. Rats recovered within half an hour of the surgery basically. After the operation, the anti-inflammatory agents levofloxacin eye drops and mydriatic agents atropine eye gel were dropped twice a day for 28 days (*Figure 1*). In order to detect intraocular infection in time, slit-lamp biological microscope was used to observe intraocular conditions.

Treatment of rat eyeballs' specimens

We observed the anterior segment of the rats using a slit-lamp biological microscope and recorded our findings at 3, 7, 14, 21, 30, 60, and 90 days. We could not know

Table 1 List of the primary antibodies used

Antibody	Dilution	Incubation	Product, manufacturer
Sirt1	1:500	1 h room temperature	ab189494, Abcam
p53	1:200		21891-1-AP, Proteintech
α -SMA	1:200		55135-1-AP, Proteintech
fn	1:100		15613-1-AP, Proteintech

Sirt1, sirtuin 1; p53, p53 tumor protein; α -SMA, alpha-smooth muscle actin; fn, fibronectin.

Table 2 General gene primer sequences

Gene	Forward	Reverse
<i>Sirt1</i>	TTTATGCTCGCCTTGCTGTG	TGTCCGGGATATATTTCCCTTTGC
<i>P53</i>	TCCGACTATACCACTATCCACTAC	GCACAAACACGAACCTCAAAG
<i>AQP 0</i>	CAGGTGACCCTGAACGAACA	GTCCGTGAGTGGGAGAATCC
γ A-crystallin	TCAACACTGACCATTTGCTGTC	CAGTCGCTGCTGCACTCATA
<i>BFSP1</i>	ACCCCGAGTTCTACTCCTCC	ATTCTCCACAGGTGGCATGG
β -Actin	AGATCAAGATCATTGCTCCTCTCT	ACGCAGCTCAGTAACAGTCC

the correspondence between the disposal sample and the situation of the anterior segment. The rats were killed humanely by cervical dislocation at 30, 60, and 90 days. Both eyeballs were removed from four rats at each time point. A 1 mL needle was used to puncture the anterior chamber at multiple points in the limbus of the cornea and the eyeballs were fixed in 4% paraformaldehyde for >24 h, then embedded in paraffin for hematoxylin and eosin (HE) and immunofluorescence staining. In addition, the regenerated lens and posterior capsule were removed intact from the eyes of 10 rats, placed in Eppendorf tubes, and stored at -80°C .

Immunofluorescence

Each slide was baked at 65°C for 1 h, dewaxed with xylene (3×10 min) and rehydrated through a graded series of ethanol solution: 100% 1×10 min, 95% 1×10 min, and rinsed in 70%. Following rehydration, the slides were rinsed in distilled water, and fixed in 10% neutral buffered formalin for 20 min. The slides were placed in a microwave for 45 s at 100% power, and then for 15 min at 20% power. After cooling, the slides were rinsed in distilled water, followed by Tris-buffered saline with Tween (TBST). The tissue sections were incubated with blocking buffer and incubated in a humidified chamber for 10 min at room

temperature. The blocking buffer was drained off and the primary antibody working solution applied (Table 1). The slides were rinsed in TBST, incubated in polymer HRP Ms+Rb (HRP labeled secondary antibody-pika mixed type) for 10 min at room temperature and then covered with reagent 50–100 μL . After rinsing in TBST, the excess wash buffer was drained off, and 100–300 μL of opal fluorophore working solution was added on to each slide for 10 min. The slides were again rinsed in TBST, and the microwave treatment was repeated. Next, 4',6-diamidino-2-phenylindole working solution was applied for 5 min at room temperature in a humidity chamber. The slides were washed in TBST buffer and water (2 min each) and finally, the coverslips were tipped onto the mounting medium. Fluorescent images were obtained using a confocal laser microscope (Leica TCS SP8 SR, Germany) and analyzed using ImageJ. Arbitrary units (AU) were used for statistical analysis of data.

Real-time fluorescence quantitative polymerase chain reaction (RT-qPCR)

We determined the relative expression of *Sirt1*, *p53*, *AQP 0*, γ A-crystallin, *BFSP1*. β -Actin was the internal reference gene; primer sequences are listed in Table 2. In addition, we detected the relative expression of miRNA-34a. U6

Table 3 miRNA primer sequence

Gene	Reverse transcriptional primers	Forward	Reverse
<i>rno-miRNA-34a-5p</i>	GTCGTATCCAGTGCCTGTCGTGGAGT CGGCAATTGCACTGGATACG	GGGTGGCAGTGTCTTAGCTG	CAGTGCGTGTGCTGGAGT
<i>U6 snRNA</i>	AACGCTTCACGAATTTGCGT	CTCGCTTCGGCAGCAC	AACGCTTCACGAATTTGCGT

miRNA, microRNA.

snRNA was the internal parameter; primer sequences are listed in *Table 3*. Total RNA was extracted from the lens and posterior capsule using the Trizol one-step method. In general, genes were subjected to reverse transcription according to the first strand synthesis kit of the Biomiga SuperRT cDNA, and miRNA reverse transcription was conducted using a Takara reverse transcription kit (20 μ L). The reaction system of RT-qPCR was 20 μ L, and the reaction system of SYBR Green PCR mixture was SYBR Mix 10 μ L, cDNA (500 ng) 1 μ L, primers for 10 μ M upstream and downstream 0.5 μ L, and ddH₂O 8 μ L. Following PCR amplification, we calculated the expression multiples of all target genes using the $2^{-\Delta\Delta CT}$ method. Using the control group as a reference, we determined the relative expression of target genes in the other three groups using the aforementioned method.

Statistical analysis

We analyzed the experimental data statistically using SPSS 25.0. Data are presented as continuous variables and were evaluated for normality using the Shapiro-Wilk test. The data are presented as mean \pm standard deviation (SD). The differences between the control and experimental groups were analyzed using the *t*-test. The differences between experimental groups at different times were analyzed using ANOVA, and the groups were pairwise compared using Tukey's multiple comparison test. Statistical significance was set at $P < 0.05$.

Results

Changes in the anterior segment

During the experiment, there was no significant anterior inflammation in the rats anterior segment because of local anti-inflammatory treatment. For each analysis, the exact value of $n=10$ in each experimental group. Following the operation, we observed the edge of the anterior capsule membrane with a slit lamp and found a clean and transparent posterior capsule membrane. After 3 days,

the membrane of the posterior capsule shrank, and the shrinkage of the posterior capsule increased after 7 days. After 14 days the near-equatorial part of the capsule was scattered with pearl corpuscles, and the shrinkage had considerably increased. After 21 days, greater mass-like proliferators accumulated irregularly inside the capsule and the equator. The central part of the posterior capsule was uneven surface for 30 days, and the surrounding area slightly protruded to form a regenerated lens. At 60 days, the central area was thicker than at 30 days, and despite the shape being similar to that of the primary lens, the transparency was poor. Compared with 60 days, the morphology and opacification of the regenerated lens was approximately the same at 90 days (*Figure 2*).

Pathological examination

HE staining revealed an intact normal lens capsule. The LECs in the inner layer of the anterior capsule were neatly arranged on the equator, but the lens fibers were arranged longitudinally. However, the posterior capsule had no cells. On day 30, the lens regenerated from the residual LECs of the equatorial region. The overall shape is fusiform, and the nucleus leaves the posterior capsule surface with the gradual elongation of the lens fibrocytes, and gradually approaches the anterior capsule. After 60 days, the fiber arrangement of the regenerated lens was similar to that of the primary lens. Furthermore, the entire regenerated lens was similar to the primary lens. The fiber arrangement and integral shape at 60 and 90 days was similar (*Figure 3*).

Immunofluorescence

Only lens and membranes were statistically analyzed. The statistical unit is AU (*Table 4, Figures 4-8*).

RT-qPCR

In the experimental group, miRNA-34a revealed a

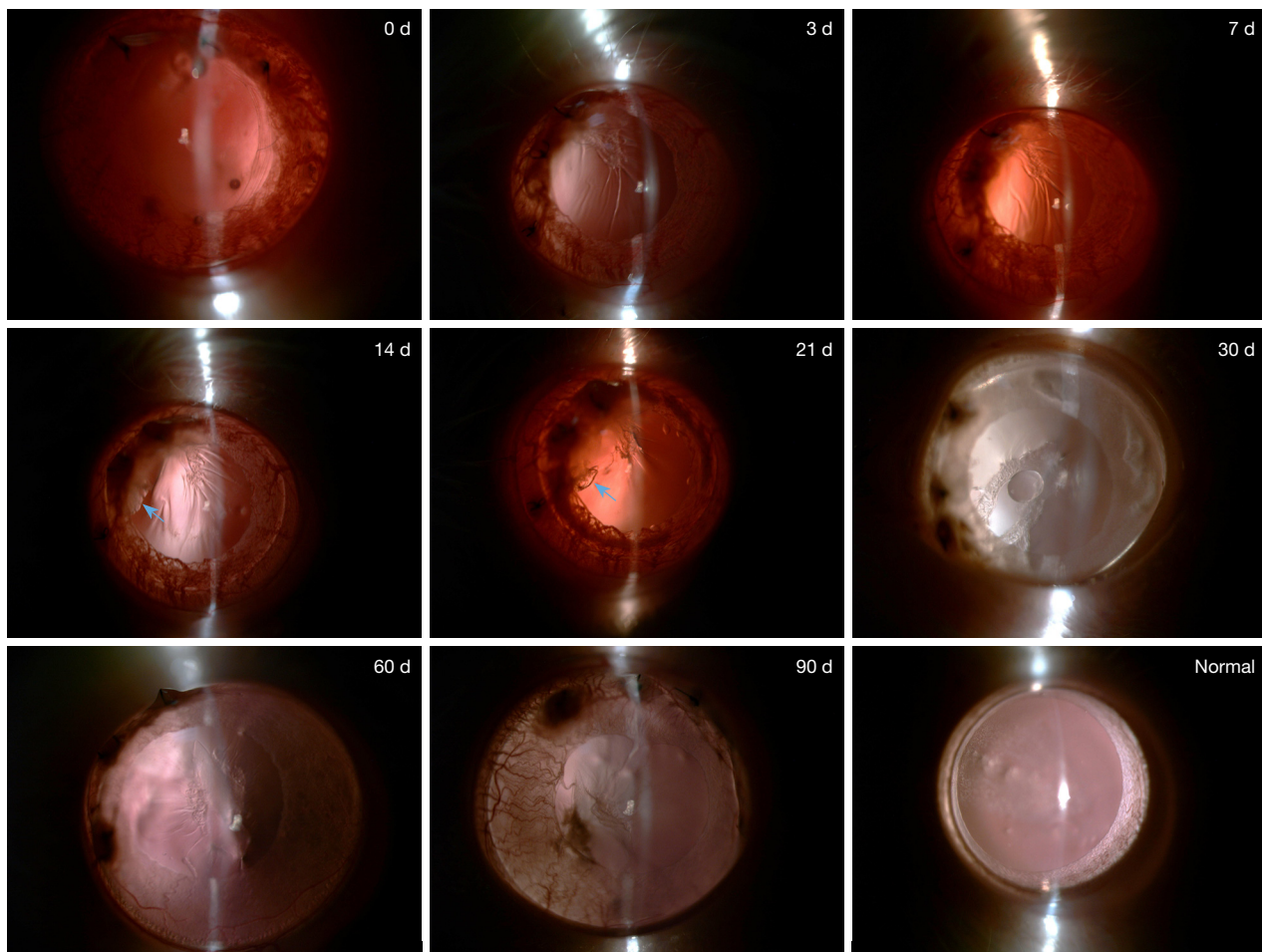


Figure 2 Slit-lamp image at each time point. The posterior capsule was clear (0 days) at the end of the extracapsular lens extraction. The shrinkage of the posterior capsule gradually increased (3 days, 7 days). Pearl corpuscles gradually appear in the posterior capsule (14 days, blue arrow), the shrinkage further increases, and the greater mass-like proliferators (21 days, blue arrow) appeared. After 30 days, the equatorial area had completely proliferated, with an irregular central area. At 60 days, the shape of the regenerated lens is similar to that of the primary lens. At 90 days, the regenerated lens depicts no obvious swelling, with uniform depth of the anterior chamber.

decreasing trend, significantly different from the normal group ($t=-23.128$, $t=-12.029$, and $t=-6.039$ on 30, 60, and 90 days, respectively; $P=0.000$). There was a significant difference in miRNA-34a levels among the three experimental groups ($F=215.581$, $P=0.000$; pairwise to pairwise ratio, $P=0.000$). Sirt1 expression significantly increased over time in comparison with the normal group ($t=10.030$, $t=13.088$, $t=3.852$ on 30, 60, and 90 days, respectively; $P<0.01$). There was a significant difference in Sirt1 levels among the experimental groups ($F=144.747$, $P=0.000$; pairwise to pairwise ratio, $P<0.01$). p53 significantly decreased over time compared with the normal group ($t=-22.379$, $t=-20.855$, $t=-13.939$ on 30, 60, and

90 days, respectively; $P=0.000$) and there was a significant difference between the experimental groups at the different time points ($F=63.387$, $P=0.000$; pairwise to pairwise ratio, $P<0.05$) (Figure 9).

AQP 0 significantly decreased over time in comparison with the normal group ($t=16.932$, $t=24.161$, $t=28.996$ on 30, 60, and 90 days, respectively; $P<0.05$) and there was a significant difference among the experimental groups ($F=41.296$, $P=0.000$; pairwise to pairwise ratio, $P=0.000$). Similarly, γ A-crystallin significantly decreased over time ($t=13.441$, $t=19.713$, $t=26.584$ on 30, 60, and 90 days, respectively; $P=0.000$), and there was a significant difference between groups ($F=145.932$, $P=0.000$; pairwise

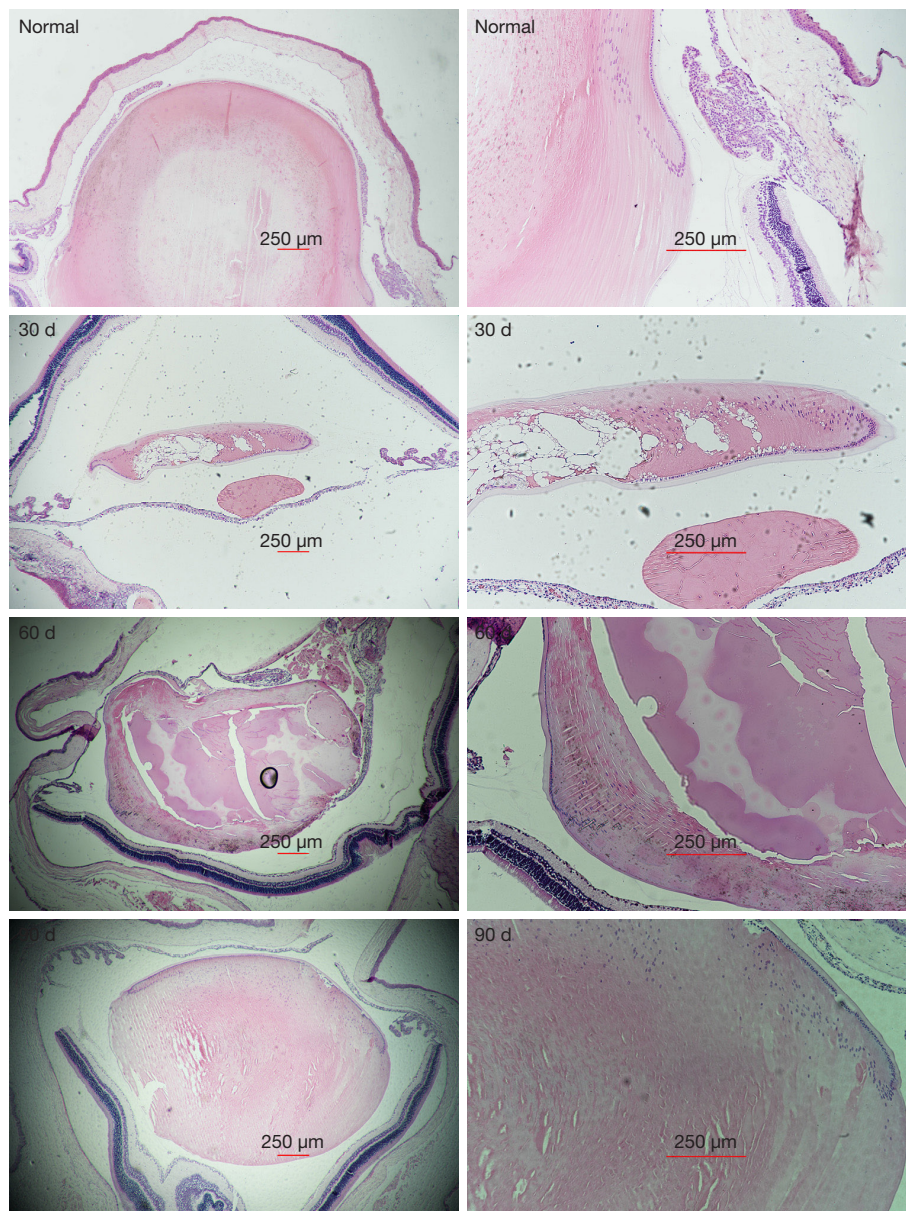


Figure 3 HE staining of a normal lens, and a regenerated lens at 30, 60, and 90 days. The normal lens fibers are arranged in order, and the single layer of LECs of the anterior capsule membrane are arranged in order to the equator. At 30 days, there was a fusiform appearance, and residual epithelial cells in the anterior sac were slightly loose. The layers of the anterior capsule at 60 days are denser, and lens fibers are arranged in order. At 90 days, the anterior capsule LECs are arranged in a monolayer similar to that of a normal lens. LECs, lens epithelial cells.

to pairwise ratio, $P < 0.01$). In contrast, no significant trend was observed for BFSP1 expression. Compared with the normal group, there were significant differences in BFSP1 levels over time ($t=15.221$, $t=24.226$, $t=18.478$, respectively; $P=0.000$), but no significant differences between experimental groups ($F=1.786$, $P=0.187$; pairwise to pairwise ratio, $P > 0.05$; *Figure 10*).

Discussion

In the present study, the residual LECs proliferated gradually over time, from the occurrence of PCO to the formation of a regenerated lens. Previous studies have shown that the volume of the lens increases linearly with the number of days after lenectomy, and that the growth

Table 4 Immunofluorescence semiquantitative expression

AU	30 d	60 d	90 d	Normal	F	P
Sirt1	55.550±10.703	124.359±4.114	140.000±2.488	31.706±1.939	777.654	0.000
p53	143.839±19.918	122.58±10.257	101.767±17.415	75.899±10.372	36.953	0.000
α -SMA	162.036±3.499	138.749±12.380	69.652±9.439	96.607±9.439	217.778	0.000
fn	140.496±17.475	157.713±19.207	165.336±17.759	175.106±16.394	6.801	0.001

Sirt1, p53, α -SMA and fn comparison within groups respectively was $P < 0.01$. AU, arbitrary units; Sirt1, sirtuin 1; p53, p53 tumor protein; α -SMA, alpha-smooth muscle actin; fn, fibronectin.

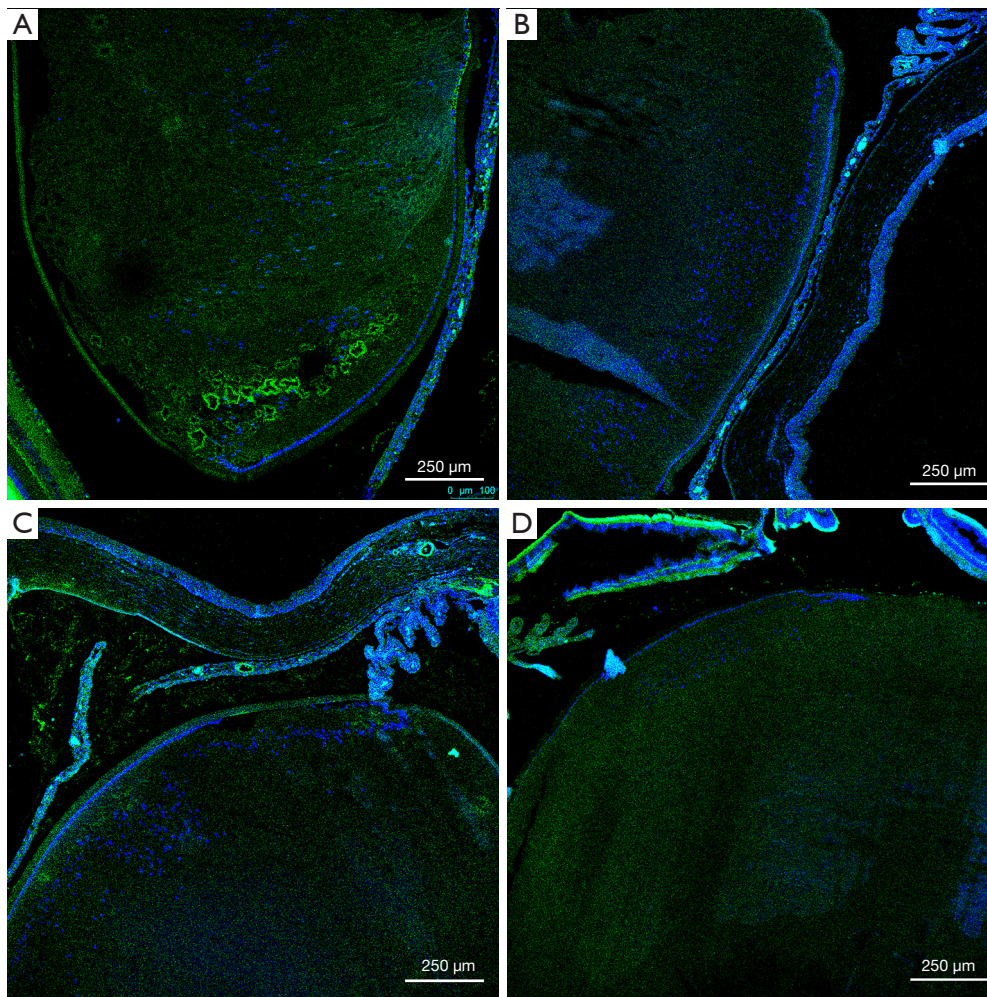


Figure 4 Sirt1 immunofluorescence. Sirt1 expression was higher in the lens epithelial cells close to the capsule. It was non-uniform in crystal fibroblasts at 30 days. Other groups are expressed as homogenized. (A) 30 days; (B) 60 days; (C) 90 days; (D) normal. Sirt1, sirtuin 1.

rate of the lens eventually decreases as the regenerated lens approaches the size of the original lens (14,30). Slit-lamp examination and HE staining revealed that a regenerated lens could be formed within 2 months after surgery. In

addition, the appearance and volume of the regenerated lens at 90 days and 60 days were similar. Nonetheless, the regenerated lens was slightly opacified, and its transparency was not comparable to that of the primary lens.

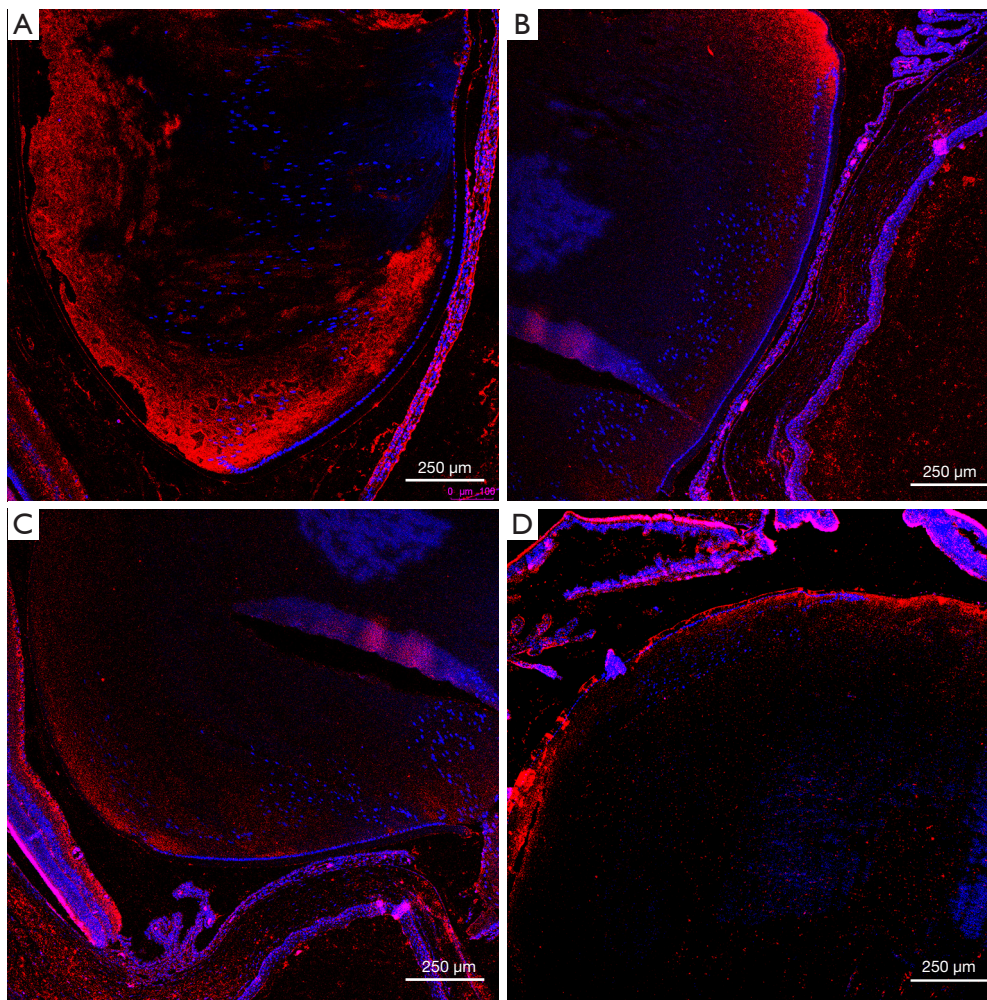


Figure 5 p53 immunofluorescence. p53 was more expressed near the capsule and the equator. Its expression decreased over time; the normal group had lower p53 levels. (A) 30 days; (B) 60 days; (C) 90 days; (D) normal. p53, tumor protein p53.

Epithelial mesenchymal transition (EMT) of LECs is the primary pathological change associated with PCO (2), and characterized by changes in cell morphology, epithelial phenotype loss, actin reorganization, and changes in interstitial cell phenotypes. α -SMA is an important marker of EMT, and a key factor in tissue fibrosis (31). Through immunofluorescence, we found that α -SMA expression was highest at 30 days, thus indicating EMT was most active at this time. Collagen and fibronectin, the primary extracellular matrix components, are distributed on the cell surface or between cells, where they form a network structure to support cell migration (31). In our study, fn expression increased gradually, concomitant with a gradual increase in cell proliferation at 90 days. Therefore, the normal volume of the lens was reached at 90 days.

We measured several lens markers. During lens development, the epithelial cells at the equator differentiate into a lens fiber cells. Moreover, mature lens fibers accumulate high concentrations of AQP 0, crystallins. AQP 0, also known as the major intrinsic protein, is the most abundant membrane protein in lens fibers (32). Cell-to-cell adhesion (CTCA) is a major function of AQP 0 and key to establishing lens transparency (33). The γ -crystallin content in the nucleus of the lens is higher than that in the cortex and the γ -crystallins are compactly arranged, thus forming a transparent tissue structure with an appropriate refractive index gradient and no scattering (34). BFSPs are lens-specific proteins belonging to the intermediate filament protein family (35). BFSP1 and BFSP2 are the major components of the beaded filaments that comprise

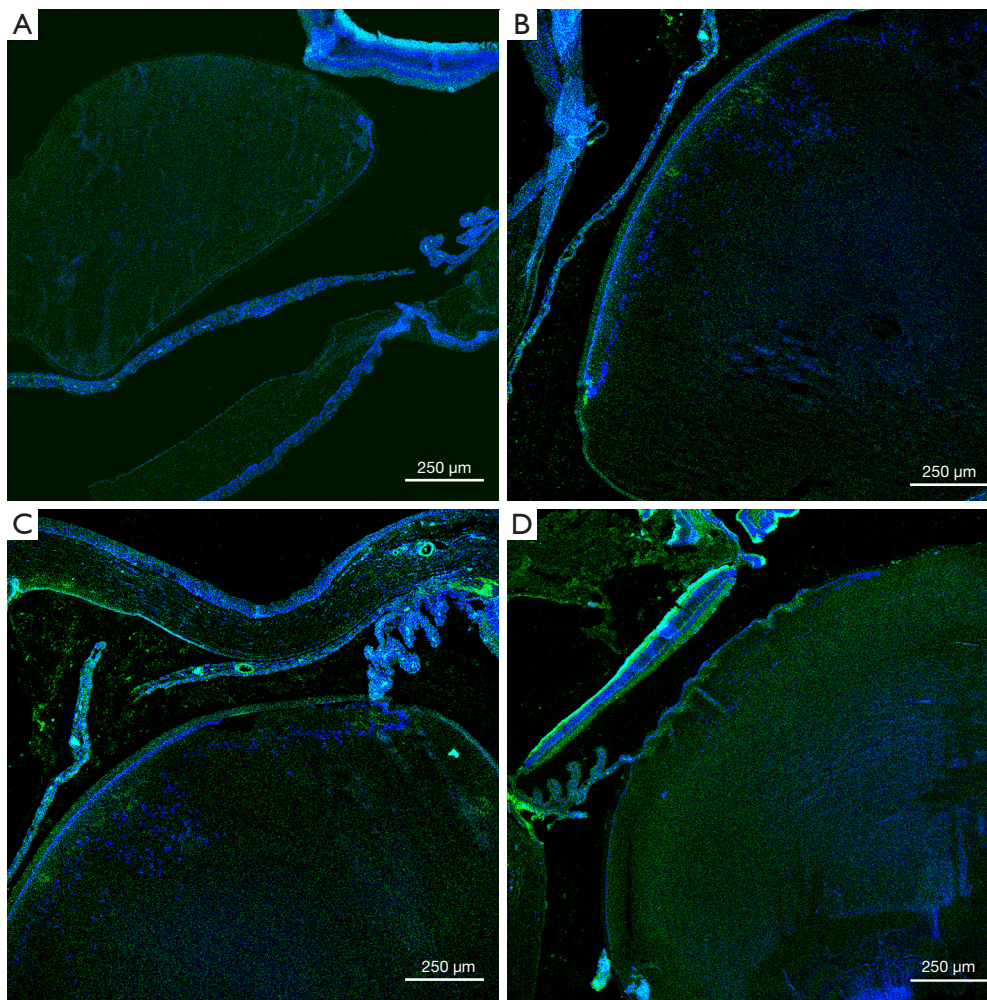


Figure 6 α -SMA immunofluorescence. α -SMA is uniformly expressed in the crystal. However, it decreases gradually over time and tends to be expressed in the lens epithelial cells close to the capsule, but at a significantly lower level than in the normal group at 90 days. (A) 30 days; (B) 60 days; (C) 90 days; (D) normal. α -SMA, alpha-smooth muscle actin.

the unique lens cytoskeleton, and play an important role in maintaining lens transparency during fetal development and fiber cell differentiation (36). In the present study, the regenerated lens was slightly turbid, and the corresponding AQP 0 and BFSP1 gene expressions were lower than in the normal group, which indicated poor CTCA and transparency of the regenerated lens. The distal promoter and the first intron of the γ A-crystallin contain the p53 binding site (37), and knocking out p53 decreases γ A-crystallin expression (37). In our experiment, p53 expression gradually decreased with increased Sirt1 expression. Moreover, γ A-crystallin expression gradually decreased, leading to decreased lens transparency.

The size and location of the capsulorhexis affect the

regeneration of the LEC lens. The smaller the diameter of the anterior capsulorhexis, the closer the transparency and the shape of the regenerated lens are to those of the normal lens; the regeneration rate is also faster, and histologically, most LECs can differentiate into well-organized lens fibers (38). If the posterior or even anterior capsular integrity can be maintained, the regenerated lens is closer to the original lens (38). In this study, in order to remove the crystal nucleus and cortex more thoroughly, a curvilinear continuous capsulorhexis with a diameter of about 2.5 mm was used. As shown in previous study (38), the posterior capsular integrity was maintained in this model, with nearly complete lens regeneration occurring within 2 months even with central capsulorhexis. The LECs of the anterior capsule

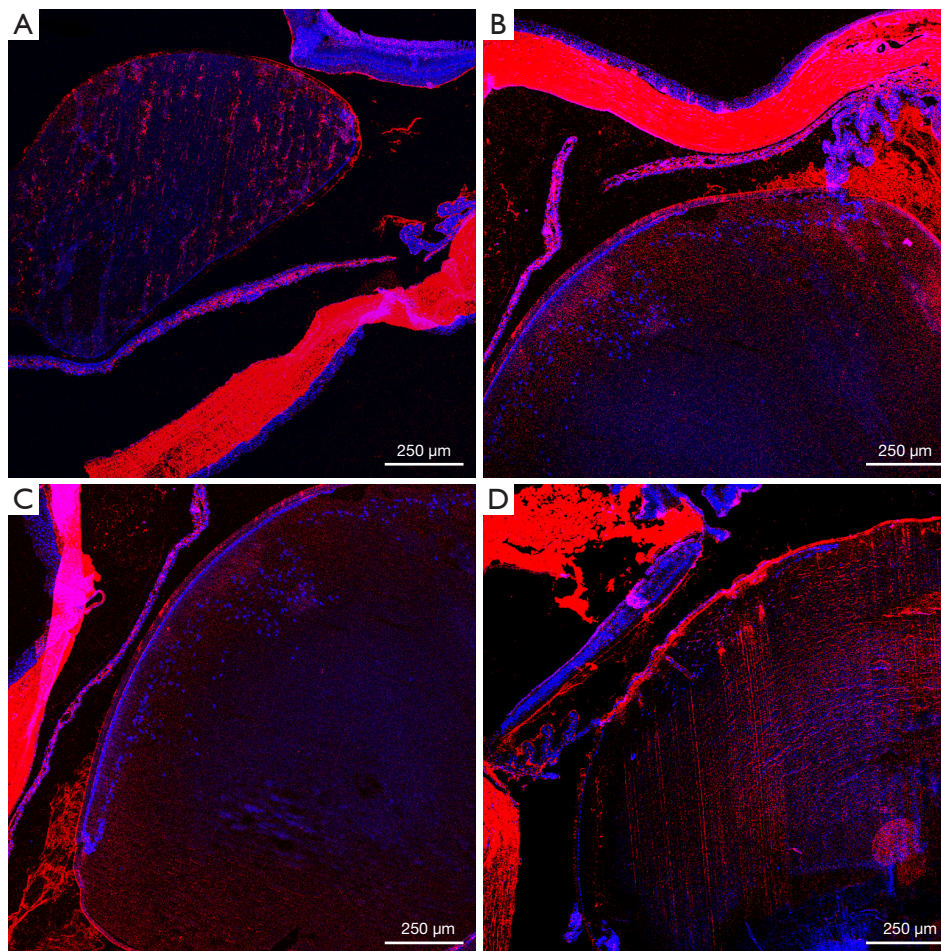


Figure 7 Fn immunofluorescence. Fn is expressed in crystal fibroblasts, with a stripe-like appearance. The expression in the normal group is higher, but that in the experimental group gradually increased over time. (A) 30 days; (B) 60 days; (C) 90 days; (D) normal. fn, fibronectin.

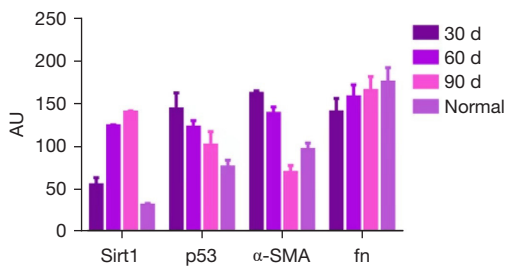


Figure 8 Immunofluorescence semiquantitative expression analysis demonstrated a gradual and significant increase in Sirt1 expression over time. Other expressions decreased gradually. However, p53 levels were still higher than normal. Although α -SMA expression was lower than normal at 90 days, it was higher than normal at 30 and 60 days. fn was always lower than normal. AU, arbitrary units; Sirt1, sirtuin 1; p53, p53 tumor protein; α -SMA, alpha-smooth muscle actin; fn, fibronectin.

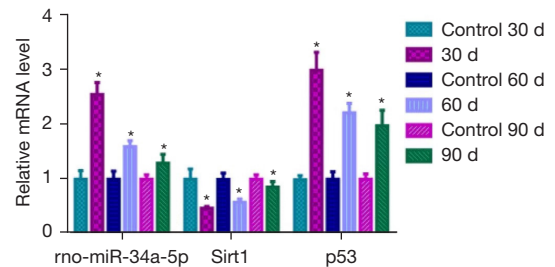


Figure 9 RT-qPCR expression of components of the miRNA-34a/Sirt1/p53 pathway. miRNA-34a negatively correlated with Sirt1, and Sirt1 negatively correlated with tumor protein p53. All factors in the pathway were significantly different at each time point between and within groups. *, $P < 0.01$. Sirt1, sirtuin 1; p53, p53 tumor protein; RT-qPCR, real-time fluorescence quantitative polymerase chain reaction.

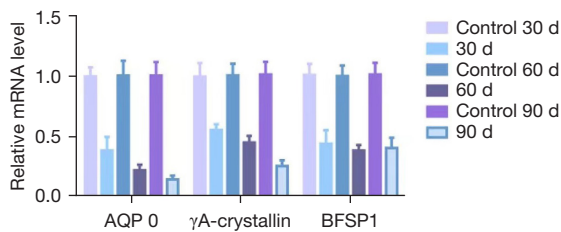


Figure 10 RT-qPCR expression of crystal markers. AQP 0 and γ A-crystallin expression were significantly different at each time point between and within groups. Beaded filament structural protein 1 was significantly different at each time point between groups. However, there was no significant difference within groups. AQP 0, aquaporin 0; BFSP1, beaded filament structural protein 1; RT-qPCR, real-time fluorescence quantitative polymerase chain reaction.

were neatly arranged, as were the lens fibers over time, although the transparency of the regenerated lens was lower than that of the primary lens. It has also been suggested that lens cells require spatial and cellular cues to initiate, sustain, and produce optically functional tissue, in addition to capsule integrity and the epithelial-fibrocyte interface (39). In order to improve the transparency of the regenerated lens, some researchers reduced the diameter of the capsulorhexis to 1.0–1.5 mm, the wound area was reduced by 1.2 mm² and moved to the periphery of the lens (15). In this study, the regenerated lens was slightly turbid. Maybe I can use this approach in further research in the future.

In the miRNA-34a/Sirt1/p53 pathway Sirt1 connects miRNA-34a and p53 in a feed-back loop (40,41). While miRNA-34a acts on Sirt1, the latter regulates p53, and both negatively correlate to cell apoptosis (42–45). To our knowledge, this is the first study to investigate the role of the miRNA-34a/Sirt1/p53 pathway in lens regeneration. To this end, we performed quantitative analyses of three target genes. miRNA-34a expression was nearly twice as high as that of the control group at 30 days, decreasing gradually over time but remaining higher than that of the normal control group at 90 days. However, Sirt1 expression increased gradually and was close to that of the normal group at 90 days. miRNA-34a expression negatively correlated with that of Sirt1, consistent with previous results (23,29). p53 expression gradually decreased with increasing Sirt1 levels, thus indicating a gradual decrease in apoptosis. This in turn maintained lens proliferation and regeneration, such that the regenerated lens was close to structure of the primary lens. Sirt1 expression in the regenerated lens was similar to that in the normal lens. Therefore, Sirt1 plays a

protective role in the maintenance of the regenerated lens.

Our experimental research can be further extended to rabbits and other mammals. But the current study has some limitations. Although rats are more genetically similar to humans, allowing for faster lens regeneration, their eyes are smaller and the lens is less transparent. In addition, we have not conducted relevant studies on Sirt1 agonists or inhibitors. Therefore, further research can be focused on this.

Conclusions

The miRNA-34a/Sirt1/p53 pathway is present in the LEC-regenerated lens. Sirt1 is a key node in the pathway and plays a protective role in lens regeneration.

Acknowledgments

Funding: This study was supported by grants from the National Natural Science Foundation of China (No. 81670837,82171024) and the Tianjin Science & Technology Foundation (No. 20JCYBJC01450). This study was also funded by Tianjin Key Medical Discipline (Specialty) Construction Project. Purchasing and raising animals, reagents required for pathology and RT-qPCR experiments are supported by funding.

Footnote

Reporting Checklist: The authors have completed the ARRIVE reporting checklist. Available at <https://atm.amegroups.com/article/view/10.21037/atm-22-2099/rc>

Data Sharing Statement: Available at <https://atm.amegroups.com/article/view/10.21037/atm-22-2099/dss>

Conflicts of Interest: All authors have completed the ICMJE uniform disclosure form (available at <https://atm.amegroups.com/article/view/10.21037/atm-22-2099/coif>). The authors have no conflicts of interest to declare.

Ethical Statement: The authors are accountable for all aspects of the work in ensuring that questions related to the accuracy or integrity of any part of the work are appropriately investigated and resolved. Animal experiments were performed under a project license (No. NKYY-DWLL-2020-098) granted by the Animal Ethical and Welfare Committees of Nankai Hospital, in compliance

with the Guide for the Care and Use of Laboratory Animals of Nankai Hospital.

Open Access Statement: This is an Open Access article distributed in accordance with the Creative Commons Attribution-NonCommercial-NoDerivs 4.0 International License (CC BY-NC-ND 4.0), which permits the non-commercial replication and distribution of the article with the strict proviso that no changes or edits are made and the original work is properly cited (including links to both the formal publication through the relevant DOI and the license). See: <https://creativecommons.org/licenses/by-nc-nd/4.0/>.

References

- Henry JJ, Hamilton PW. Diverse Evolutionary Origins and Mechanisms of Lens Regeneration. *Mol Biol Evol* 2018;35:1563-75.
- Sugiyama Y, Nakazawa Y, Sakagami T, et al. Capsaicin attenuates TGF β 2-induced epithelial-mesenchymal-transition in lens epithelial cells in vivo and in vitro. *Exp Eye Res* 2021;213:108840.
- Karahan E, Er D, Kaynak S. An Overview of Nd:YAG Laser Capsulotomy. *Med Hypothesis Discov Innov Ophthalmol* 2014;3:45-50.
- Gu Y, Yao K, Fu Q. Lens regeneration: scientific discoveries and clinical possibilities. *Mol Biol Rep* 2021;48:4911-23.
- Inoue T, Inoue R, Tsutsumi R, et al. Lens regenerates by means of similar processes and timeline in adults and larvae of the newt *Cynops pyrrhogaster*. *Dev Dyn* 2012;241:1575-83.
- Powell JA, Powers C. Effect on lens regeneration of implantation of spinal ganglia into the eyes of the newt, *Notophthalmus*. *J Exp Zool* 1973;183:95-118.
- Reyer RW. The influence of neural retina and lens on lens regeneration from dorsal iris implants in *Triturus viridescens* larvae. *Dev Biol* 1966;14:214-45.
- Reyer RW. DNA synthesis and the incorporation of labeled iris cells into the lens during lens regeneration in adult newts. *Dev Biol* 1971;24:533-58.
- Freeman G. Lens regeneration from the cornea in *Xenopus laevis*. *J Exp Zool* 1963;154:39-65.
- Perry KJ, Thomas AG, Henry JJ. Expression of pluripotency factors in larval epithelia of the frog *Xenopus*: evidence for the presence of cornea epithelial stem cells. *Dev Biol* 2013;374:281-94.
- Hamilton PW, Henry JJ. The lens regenerative competency of limbal vs. central regions of mature *Xenopus* cornea epithelium. *Exp Eye Res* 2016;152:94-9.
- Gwon A, Enomoto H, Horowitz J, et al. Induction of de novo synthesis of crystalline lenses in aphakic rabbits. *Exp Eye Res* 1989;49:913-26.
- Gwon A, Gruber LJ, Mantras C. Restoring lens capsule integrity enhances lens regeneration in New Zealand albino rabbits and cats. *J Cataract Refract Surg* 1993;19:735-46.
- Zhou KJ, Li YN, Huang FR, et al. In Vivo Observation of Lens Regeneration in Rat Using Ultra-Long Scan Depth Optical Coherence Tomography. *Invest Ophthalmol Vis Sci* 2016;57:6615-23.
- Lin H, Ouyang H, Zhu J, et al. Lens regeneration using endogenous stem cells with gain of visual function. *Nature* 2016;531:323-8.
- Hayashi T, Mizuno N, Ueda Y, et al. FGF2 triggers iris-derived lens regeneration in newt eye. *Mech Dev* 2004;121:519-26.
- Fukui L, Henry JJ. FGF signaling is required for lens regeneration in *Xenopus laevis*. *Biol Bull* 2011;221:137-45.
- Hayashi T, Mizuno N, Takada R, et al. Determinative role of Wnt signals in dorsal iris-derived lens regeneration in newt eye. *Mech Dev* 2006;123:793-800.
- Malloch EL, Perry KJ, Fukui L, et al. Gene expression profiles of lens regeneration and development in *Xenopus laevis*. *Dev Dyn* 2009;238:2340-56.
- Tsonis PA, Tsavaris M, Call MK, et al. Expression and role of retinoic acid receptor alpha in lens regeneration. *Dev Growth Differ* 2002;44:391-4.
- Thomas AG, Henry JJ. Retinoic acid regulation by CYP26 in vertebrate lens regeneration. *Dev Biol* 2014;386:291-301.
- Maki N, Martinson J, Nishimura O, et al. Expression profiles during dedifferentiation in newt lens regeneration revealed by expressed sequence tags. *Mol Vis* 2010;16:72-8.
- Li QL, Zhang HY, Qin YJ, et al. MicroRNA-34a promoting apoptosis of human lens epithelial cells through down-regulation of B-cell lymphoma-2 and silent information regulator. *Int J Ophthalmol* 2016;9:1555-60.
- Li L. Regulatory mechanisms and clinical perspectives of miR-34a in cancer. *J Cancer Res Ther* 2014;10:805-10.
- Thor T, Künkele A, Pajtlér KW, et al. MiR-34a deficiency accelerates medulloblastoma formation in vivo. *Int J Cancer* 2015;136:2293-303.
- Xu Y, Li F, Lv L, et al. Oxidative stress activates SIRT2 to deacetylate and stimulate phosphoglycerate mutase. *Cancer Res* 2014;74:3630-42.

27. Conrad E, Polonio-Vallon T, Meister M, et al. HIPK2 restricts SIRT1 activity upon severe DNA damage by a phosphorylation-controlled mechanism. *Cell Death Differ* 2016;23:110-22.
28. Xiu C, Jiang J, Song R. Expression of miR-34a in cataract rats and its related mechanism. *Exp Ther Med* 2020;19:1051-7.
29. Zheng T, Lu Y. SIRT1 Protects Human Lens Epithelial Cells Against Oxidative Stress by Inhibiting p53-Dependent Apoptosis. *Curr Eye Res* 2016;41:1068-75.
30. Chen W, Tsissios G, Sallèse A, et al. In Vivo Imaging of Newt Lens Regeneration: Novel Insights Into the Regeneration Process. *Transl Vis Sci Technol* 2021;10:4.
31. Ma B, Jing R, Liu J, et al. CTGF Contributes to the Development of Posterior Capsule Opacification: an in vitro and in vivo study. *Int J Biol Sci* 2018;14:437-48.
32. Gu S, Biswas S, Rodriguez L, et al. Connexin 50 and AQP0 are Essential in Maintaining Organization and Integrity of Lens Fibers. *Invest Ophthalmol Vis Sci* 2019;60:4021-32.
33. Varadaraj K, Kumari SS. Molecular mechanism of Aquaporin 0-induced fiber cell to fiber cell adhesion in the eye lens. *Biochem Biophys Res Commun* 2018;506:284-9.
34. Vendra VP, Khan I, Chandani S, et al. Gamma crystallins of the human eye lens. *Biochim Biophys Acta* 2016;1860:333-43.
35. Wang H, Zhang T, Wu D, et al. A novel beaded filament structural protein 1 (BFSP1) gene mutation associated with autosomal dominant congenital cataract in a Chinese family. *Mol Vis* 2013;19:2590-5.
36. Alizadeh A, Clark J, Seeberger T, et al. Targeted deletion of the lens fiber cell-specific intermediate filament protein filensin. *Invest Ophthalmol Vis Sci* 2003;44:5252-8.
37. Hu XH, Nie Q, Yi M, et al. The tumor suppressor, p53 regulates the γ A-crystallin gene during mouse lens development. *Curr Mol Med* 2014;14:1197-204.
38. Tan X, Liu Z, Zhu Y, et al. The Fate of In Situ Lens Regeneration is Determined by Capsulorhexis Size. *Curr Mol Med* 2017;17:270-9.
39. Wu W, Lois N, Prescott AR, et al. The importance of the epithelial fibre cell interface to lens regeneration in an in vivo rat model and in a human bag-in-the-lens (BiL) sample. *Exp Eye Res* 2021;213:108808.
40. Lou G, Liu Y, Wu S, et al. The p53/miR-34a/SIRT1 Positive Feedback Loop in Quercetin-Induced Apoptosis. *Cell Physiol Biochem* 2015;35:2192-202.
41. Xia C, Shui L, Lou G, et al. 0404 inhibits hepatocellular carcinoma through a p53/miR-34a/SIRT1 positive feedback loop. *Sci Rep* 2017;7:4396.
42. Yan S, Wang M, Zhao J, et al. MicroRNA-34a affects chondrocyte apoptosis and proliferation by targeting the SIRT1/p53 signaling pathway during the pathogenesis of osteoarthritis. *Int J Mol Med* 2016;38:201-9.
43. Xiong H, Pang J, Yang H, et al. Activation of miR-34a/SIRT1/p53 signaling contributes to cochlear hair cell apoptosis: implications for age-related hearing loss. *Neurobiol Aging* 2015;36:1692-701.
44. Ye Z, Fang J, Dai S, et al. MicroRNA-34a induces a senescence-like change via the down-regulation of SIRT1 and up-regulation of p53 protein in human esophageal squamous cancer cells with a wild-type p53 gene background. *Cancer Lett* 2016;370:216-21.
45. Heydari H, Ghiasi R, Hamidian G, et al. Voluntary exercise improves sperm parameters in high fat diet receiving rats through alteration in testicular oxidative stress, mir-34a/SIRT1/p53 and apoptosis. *Horm Mol Biol Clin Investig* 2021;42:253-63.

Cite this article as: Bi X, Wang R, Song H, Wang Y, Hao P, Li X. The miRNA-34a/Sirt1/p53 pathway in a rat model of lens regeneration. *Ann Transl Med* 2022;10(11):636. doi: 10.21037/atm-22-2099